

Dynamical singlets and correlation-assisted Peierls transition in VO₂

S. Biermann,^{1,2} A. Poteryaev,^{3,1} A. I. Lichtenstein,⁴ and A. Georges^{1,2}

¹*Centre de Physique Théorique, Ecole Polytechnique, 91128 Palaiseau Cedex, France*

²*LPS, Université Paris Sud, Bât. 510, 91405 Orsay, France*

³*University of Nijmegen, NL-6525 ED Nijmegen, The Netherlands*

⁴*Institut für Theoretische Physik, Universität Hamburg, Jungiusstrasse 9, 20355 Hamburg, Germany*

A theory of the metal-insulator transition in vanadium dioxide from the high-temperature rutile to the low-temperature monoclinic phase is proposed on the basis of cluster dynamical mean field theory, in conjunction with the density functional scheme. The interplay of strong electronic Coulomb interactions and structural distortions, in particular the dimerization of vanadium atoms in the low temperature phase, plays a crucial role. We find that VO₂ is *not* a conventional Mott insulator, but that the formation of dynamical V-V singlet pairs due to strong Coulomb correlations is necessary to trigger the opening of a Peierls gap.

PACS numbers: 71.27.+a, 71.30.+h, 71.15.Ap

Vanadium dioxide (VO₂) undergoes a first-order transition from a high-temperature metallic phase to a low-temperature insulating phase [1] at almost room-temperature ($T = 340$ K). The resistivity jumps by several orders of magnitude through this transition, and the crystal structure changes from rutile (R-phase) at high-temperature to monoclinic (so-called M₁-phase) at low-temperature. The latter is characterized by a dimerization of the vanadium atoms into pairs, as well as a tilting of these pairs with respect to the c-axis.

Whether these structural changes are solely responsible for the insulating nature of the low-T phase, or whether correlation effects also play a role, has been a subject of much debate. The strong dimerization, as well as the fact that the insulating phase is non-magnetic suggests that VO₂ might be a typical case of a Peierls insulator. However, pioneering experimental work by Pouget *et al.* demonstrated that minute amounts of Cr-substitutions [2], as well as, remarkably, uniaxial stress applied to *pure* VO₂ [3] leads to a new phase (M₂) in which only half of the V-atoms dimerize, while the other half forms chains of equally-spaced atoms behaving as spin-1/2 Heisenberg chains. That this phase is also insulating strongly suggests that the physics of VO₂ is very close to that of a Mott-Hubbard insulator. Zylbersztein and Mott [4], Sommers and Doniach [5] and Rice *et al.* [6] suggested that Coulomb repulsion indeed plays a major role in opening the insulating gap.

The main qualitative aspects of the electronic structure of VO₂ have been explained long ago by Goodenough [7]. In the rutile structure (space group $P4_2/mnm$), the V atoms are surrounded by O octahedra forming an edge-sharing chain along the c-axis. The d -levels of the V-ions are split into lower lying t_{2g} states and e_g^σ states. The latter lie higher in energy and are therefore empty. The tetragonal crystal field further splits the t_{2g} multiplet into an a_{1g} state and an e_g^π doublet ($d_{||}$ and π^* states, respectively in the terminology of Ref. [7]). The a_{1g} orbitals are directed along the c-axis, with good σ -bonding of the V-V

pair along this direction. In the monoclinic phase (space group $P2_1/c$), the dimerization and tilting of the V-V pairs results in two important effects. First, the a_{1g} ($d_{||}$) band is split into a lower-energy bonding combination and a higher-energy antibonding one. Second, the V_d-O_p antibonding e_g^π (π^*) states are pushed higher in energy, due to the tilting of the pairs which increases the overlap of these states with O states. In Goodenough's picture, the single d-electron occupies the $d_{||}$ -bonding combination, resulting in a (Peierls-like) band gap.

Electronic structure calculations based on density functional theory within the local density approximation (DFT-LDA) have since provided support for this qualitative description in terms of molecular orbitals (see the recent work of Eyert [8] for an extensive discussion and references). Molecular dynamics calculations by Wentzcovich *et al.* [9] with variable cell shape successfully found the M₁ structure to have the lowest total energy, with structural parameters in reasonable agreement with experiment. DFT-LDA calculations fail however to yield the opening of the band gap: the top of the bonding $d_{||}$ -band is found to overlap slightly with the bottom of the π^* -band (only for a hypothetical structure with larger dimerizations would the band gap fully open). Not surprisingly, recent DFT-LDA calculations of the M₂ phase [8] also fail in producing an insulator.

This discussion makes clear that only a theoretical treatment in which structural aspects as well as correlations within V-V pairs are taken into account on equal footing, is able to successfully decide on the underlying mechanism for the metal-insulator transition in VO₂. In this Letter, we fulfill this goal by using a cluster extension of dynamical mean-field theory (C-DMFT) [10] in combination with state-of-the-art DFT-LDA calculations within the recently developed Nth-order muffin-tin orbital (NMTO) [11] implementation. This allows for a consistent description of both the metallic rutile phase and the insulating monoclinic phase. We find that the insulating state can be viewed as a molecular solid of singlet

dimers in the Heitler-London (correlated) limit. While a description in terms of renormalised Peierls bands is possible at low-energy, broad Hubbard bands are present at higher energy. Recent photoemission experiments can be successfully interpreted on the basis of our results, which also yield specific predictions for inverse-photoemission spectra.

Previous theoretical work on VO₂ based on DMFT has recently appeared [12, 13]. These works, however, are based on a single-site DMFT approach. This is appropriate in the metallic phase, but not in the insulating phase. While we do find that by increasing U to unphysically high values, a Mott insulator can be induced in a single-site DMFT approach, the formation of singlet pairs resulting from the strong dimerization can only be captured in a cluster extension of DMFT in which the dimers are taken as the key unit. Only then can a non-magnetic insulator with a spin-gap be obtained, in agreement with experiments. C-DMFT allows for a consistent extension to the solid-state of the simple Heitler-London picture of an isolated molecule. Electrons can be shared between all singlets through the self-consistent electronic bath, resulting in a “dynamical singlets” description.

Given the filling of one d-electron per vanadium, and the crystal-field splitting separating the t_{2g} and e_g^σ states in both phases, it is appropriate to work within a set of localized V-centered t_{2g} Wannier-orbitals, and to neglect the degrees of freedom from all other bands. As in Ref. [14], our Wannier orbitals are orthonormalized NMTOs, which have all partial waves other than V- d_{xy} , d_{yz} and d_{zx} downfolded. These notations refer to the *local coordinate axes* ($z \parallel [110]$) attached to a given V atom surrounding the oxygen octahedron. DFT-LDA calculations followed by this downfolding procedure yield a Hamiltonian matrix $H_{mm'}^{\text{LDA}}(\mathbf{k})$ (of size 6×6 in the rutile phase, which has 2 V-atoms per unit cell, and 12×12 in the monoclinic phase, with 4 V atoms per unit cell). Our results for the DFT-LDA electronic structure in both phases are in agreement with previously published studies, and with the qualitative picture described above. The partial densities of states for the $a_{1g} \equiv d_{xy}$ and $e_g^\pi \equiv \{d_{yz}, d_{xz}\}$ are presented in Fig. 1 and Fig. 2 for the rutile and monoclinic phases, respectively. The total t_{2g} bandwidth is almost the same for both phases ($\sim 2.59\text{eV}$ in rutile and $\sim 2.56\text{eV}$ in monoclinic). In the rutile phase, the single d-electron is almost equally distributed between all three orbital components within LDA (0.36 in a_{1g} and 0.32 in each of the e_g^π 's). From the Hamiltonian matrix in real space, we can extract the hopping integrals between V centers. The largest one, $t_{xy,xy} = -0.31\text{eV}$ is between a_{1g} orbitals forming chains along the c-axis, but the hoppings $t_{xz,yz}$ within the chains and $t'_{yz,yz}, t'_{xz,xz}$ are only twice smaller (0.17 – 0.19eV). Given that there are 8 next-nearest neighbours of this type, and only 2 along the chains, the properties of the rutile metal are therefore fairly isotropic. The electronic structure dras-

tically changes in the monoclinic phase (Fig. 2). The a_{1g} state is split into a bonding combination below the Fermi level, and an antibonding combination higher in energy. The splitting between the bonding and antibonding states is set by the intra-dimer hopping, which we find to be $t_{xy,xy}^{\text{intra}} = -0.68\text{eV}$, hence a splitting of order $2t_{xy,xy} \sim 1.4\text{eV}$. The two a_{1g} peaks in the density of states (DOS) are very narrow, corresponding to the very small inter-dimer hopping $t_{xy,xy}^{\text{inter}} \simeq -0.03\text{eV}$. The intra-dimer hopping is by far the dominant one in this phase, with the second largest being $t'_{xz,yz}$ in the [111] direction ($\sim 0.22\text{eV}$) and all others much smaller. Also, the e_g^π states are pushed higher in energy in the monoclinic phase, so that the LDA occupancies are now 0.74 for the a_{1g} (bonding) band and only 0.12 and 0.14 for the d_{yz} and d_{xz} , respectively. Still, these bands overlap weakly and the LDA fails to open the insulating gap ($\sim 0.6\text{eV}$ experimentally).

We use the LDA-NMTO Hamiltonian $H_{mm'}^{\text{LDA}}(\mathbf{k})$ as a starting point for the construction of a multi-band Hubbard Hamiltonian of the form of Eq. (1) in Ref. [14] involving direct and exchange terms of the screened *on-site* Coulomb interaction $U_{mm'}$ and $J_{mm'}$, with the parametrization $U_{mm} = U$, $U_{mm'} = U - 2J$ and $J_{mm'} = J$ for $m \neq m'$. We assume double counting corrections to be orbital-independent within the t_{2g} manifold, thus resulting in a simple shift of the chemical potential. Recently, it has become feasible to solve this many-body Hamiltonian using the dynamical mean-field approximation (DMFT) and to obtain realistic physical properties, even when all off-diagonal terms in orbital space in the local self-energy $\Sigma_{mm'}$ are retained [14]. Here, we go one step further by including also non-local terms in the self-energy. The latter are constructed from a cluster LDA+DMFT treatment [15]. More precisely, instead of calculating the self-energy from a local impurity model embedding one single atom in a self-consistent bath, a *pair* of V atoms in the complex bath is explicitly considered. The self-energy $\Sigma_{mm'}^{i_c j_c}$ and (Weiss) dynamical mean-field $\mathcal{G}_{mm'}^{i_c j_c}$ become matrices in both the orbital indices $m, m' = (xy, yz, xz)$ and the intra-dimer site indices $i_c, j_c = 1, 2$. The inter-dimer components of the self-energy as well as long-range correlations are neglected in this C-DMFT scheme. Using the crystal symmetries in the monoclinic phase, a 12×12 block-diagonal self-energy matrix is constructed from the 6×6 matrix $\Sigma_{mm'}^{i_c j_c}$, so that the C-DMFT approximation to the self-energy takes in this case the form :

$$\Sigma = \begin{pmatrix} \hat{\Sigma}_{11} & \hat{\Sigma}_{12} & 0 & 0 \\ \hat{\Sigma}_{21} & \hat{\Sigma}_{22} & 0 & 0 \\ 0 & 0 & \hat{\Sigma}_{11} & \hat{\Sigma}_{12} \\ 0 & 0 & \hat{\Sigma}_{21} & \hat{\Sigma}_{22} \end{pmatrix} \quad (1)$$

where $\hat{\Sigma}_{12}$ [$\hat{\Sigma}_{11}$] denotes the 3×3 intersite [on-site] self-energy matrix in the space of the t_{2g} orbitals. This is then

combined with $H_{mm'}^{\text{LDA}}(\mathbf{k})$ in order to obtain the Green's function at a given \mathbf{k} -point. After summation over \mathbf{k} , the intra-dimer block of the Green's function $G_{mm'}^{i_e j_e}$ is extracted and used in the C-DMFT self-consistency condition. The 6-orbital impurity problem is solved by a numerically exact quantum Monte Carlo (QMC) scheme using up to 100 slices in imaginary time at temperatures down to 770 K. From the Green's function on the imaginary-time axis we calculate the spectral function by using the maximum entropy technique.

We first discuss our results for the rutile phase (Fig. 1). In this phase, we found that the results of single-site and cluster-DMFT calculations are indistinguishable for all practical purposes. Correlations reduce the *total* (occupied and unoccupied) bandwidth corresponding to the coherent part of the spectral density from 2.59 eV in LDA down to about 1.8 eV (see Fig. 1). This is consistent with the quasiparticle weight that we extract from the self-energy: $Z \simeq 0.66$. Hence, the metallic phase of VO_2 can be characterized as a metal with an intermediate level of correlations. We observe however, that the *occupied bandwidth* is barely modified ($\sim 0.5\text{eV}$ in both the LDA and our results). This finding is in agreement with photoemission experiments [16, 17], and our work demonstrates that it is compatible with a local self-energy. A prominent quasi-particle coherence peak is found close to the Fermi level. This has recently been demonstrated experimentally in high photon energy bulk-sensitive photoemission experiments [17] (and is also suggested by low-photon energy PES provided surface contributions are subtracted [16]). Hubbard bands are apparent at higher energies, with a rather weak lower Hubbard band about -1.5 eV below the Fermi level and a more pronounced upper Hubbard band at about $+2.5 - 3$ eV. The former has been observed in photoemission experiments [16, 17, 18], while the latter constitutes a prediction for BIS experiments. Finally, correlations result in a slight increase of the occupancy of the a_{1g} band (0.42) relative to the e_g^π ones (0.29, 0.29), in comparison to LDA: (0.36; 0.32, 0.32).

Figure 2 displays the spectral functions for the monoclinic phase calculated within cluster-DMFT in comparison with the LDA DOS. The key point is that inclusion of non-local self-energy effects succeeds in opening up a gap of about 0.6 eV, in reasonable agreement with experiments. Our calculations also yield a large redistribution of the electronic occupancies in favor of the a_{1g} orbital which now carries 0.8 electrons per vanadium (with only $\sim (0.1, 0.1)$ remaining in the e_g^π orbitals). This charge redistribution is a common feature of many models of VO_2 , whether correlations- or band-driven, and is also observed in experiments. In the present context, the fact that the single electron occupies almost entirely the a_{1g} orbital, together with the fact that U is larger than the intra-dimer hopping (itself much bigger than other hoppings), means that the ground-state of each dimer is close

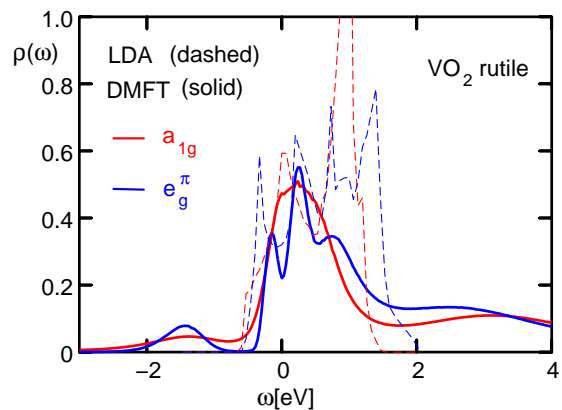


FIG. 1: Spectral function for the rutile phase as calculated within DMFT with $U = 4\text{eV}$, $J = 0.68\text{eV}$ (solid lines) in comparison to the LDA DOS (dashed lines). The red (blue) lines show the partial contributions of the a_{1g} (e_g^π) bands.

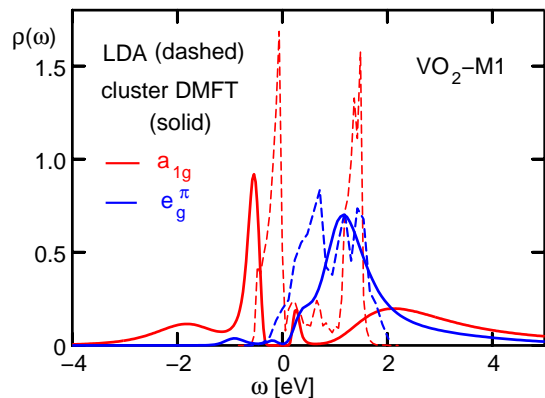


FIG. 2: Spectral function for the monoclinic phase as calculated within cluster-DMFT with $U = 4\text{eV}$, $J = 0.68\text{eV}$ (solid lines) in comparison to the LDA DOS (dashed lines). The red [blue] lines show the partial contributions of the a_{1g} [e_g^π (averaged)] bands.

to the Heitler-London limit. In this limit, one has two electrons with opposite spins on each site forming a singlet state, rather than an uncorrelated wave-function in which two electrons (per dimer) are placed in the bonding combination of atomic orbitals (hence a large double occupancy). The transition into the insulating state is facilitated by the Heitler-London stabilisation energy. This confirms the early proposal of Sommers and Doniach [5]. As a result, the dominant excitation when adding an electron *in the a_{1g} orbital* costs an energy which is set by U . This is apparent on our spectra: the antibonding combination of a_{1g} orbitals corresponding to the narrow peak at $\sim +1.5$ eV present in the LDA calculation is replaced by a broad upper Hubbard band centered at $\sim +2.2$ eV

(the precise value of course depends on the choice of U). Correspondingly, there is a (weak) lower Hubbard band at ~ -1.8 eV. The *low-energy* nature of this singlet insulator, however, is quite different from that of a standard Mott insulator in which local moments are formed in the insulating state. This is manifested by the fact that the low-frequency behaviour of the on-site component of the self-energy associated with the a_{1g} orbital (Fig. 3) is linear in frequency $\Sigma_{11} = \Sigma_{11}(0) + (1 - 1/Z_i)\omega + \dots$, in contrast to the local-moment Mott insulator in which $\Sigma_{11} \propto 1/\omega$ diverges. As a result, the spectrum displays a narrow a_{1g} peak, at an energy ~ -0.8 eV below the gap, which carries most of the spectral weight for $\omega < 0$. This peak should not be interpreted as an incoherent lower Hubbard band, but rather as a quasiparticle which has been gapped out (Z_i can be interpreted as the spectral weight of the gapped low-energy quasiparticle in the insulator). Hence, at low-energy, the physics is that of a renormalised Peierls insulator (analogously, a correlated Kondo insulator can be viewed as a renormalised hybridisation-gap insulator at low-energy). The bonding-antibonding splitting is renormalized down by correlations. Indeed, a weaker a_{1g} peak is visible in our spectra at the upper gap edge, at an energy considerably smaller than the antibonding peak in the LDA DOS. The e_g^π band, in contrast to the a_{1g} , is weakly correlated, as evident from the self-energy in Fig. 3 and expected from the low electron occupancy. Its bottom lies in the same energy range than the ‘‘renormalised’’ antibonding peak, so that the gap can as well be considered to open between the a_{1g} and the e_g^π band.

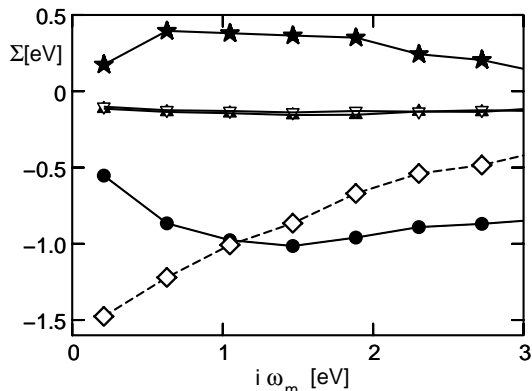


FIG. 3: Self-energies $\Sigma(i\omega_n)$ from the C-DMFT calculation (for $U=4$ eV, $J=0.68$ eV) for the M_1 phase, at low (imaginary) frequency. Circles [triangles]: imaginary part of the on-site diagonal a_{1g} [e_g^π] component. Diamonds [stars]: real [imaginary] part of the inter-site a_{1g} component.

Our findings for the spectral function explain the recent photoemission data of T. Koethe *et al.* [17]. These authors made the puzzling observation that a prominent peak below the gap appears in the insulator but at an

energy (~ -0.8 eV) which is shifted *towards positive energy* in comparison to the (weak) lower Hubbard band measured in the metallic phase (~ -1.2 eV). We propose that this peak is actually the coherent quasiparticle peak at the bottom of the gap, rather than the lower Hubbard band. The latter is present at higher (negative) energy but remains rather weak even in the insulator. Fig. 4 compares the total t_{2g} spectral functions calculated for the metallic and the insulating phases.

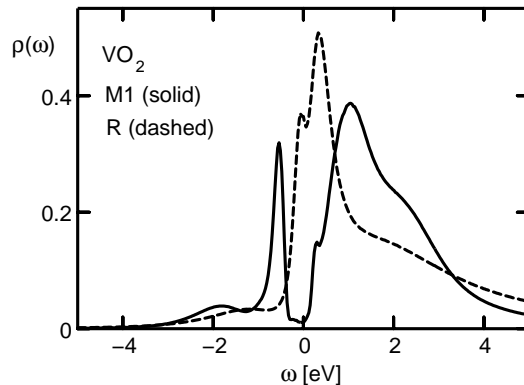


FIG. 4: Spectral function of the t_{2g} orbitals for rutile and monoclinic phases as calculated within DMFT/cluster-DMFT with $U = 4$ eV, $J = 0.68$ eV. The Hubbard band in the rutile phase is located at about -1.2 eV, whereas the pronounced peak at -0.8 eV in the monoclinic phase corresponds to the gapped quasi-particle (see text).

Finally, let us mention that we have discussed the results obtained for a specific choice of the interaction parameters $U = 4$ eV and $J = 0.68$ eV. We have actually performed calculations for other choices. In particular, we found that it is possible to stabilize an insulating state within C-DMFT for smaller values of U (e.g $U = 2$ eV), but only if the Hund’s coupling J is taken to be small (in which case it is easier to redistribute the charge towards the a_{1g} orbital). Also, we emphasize that a *single-site* DMFT calculation can lead to an insulating state for rather large values of U ($U \geq 5$ eV). However, this insulating solution is a conventional Mott insulator with a local moment, and therefore would display a large magnetic susceptibility which does not correspond to the actual physics of insulating VO_2 .

In conclusion, we have presented LDA+CDMFT calculations for vanadium dioxide. Both the metallic rutile phase and the insulating monoclinic phase are correctly captured by this approach.

We are grateful to J-P. Pouget, C. Noguera, F. Finocchi, V. Eyert, A. Fujimori and L.H. Tjeng for useful discussions, and to the KITP Santa Barbara for hospitality and support (NSF Grant PHY99-07949). S.B and A.G acknowledge funding from CNRS and Ecole Polytechnique, and A.P from FOM. Computing time was provided

by IDRIS (Orsay) under project No. 041393.

-
- [1] F. J. Morin, Phys. Rev. Lett. **3**, 34 (1959).
 [2] J. P. Pouget, et al. Phys. Rev. B **10**, 1801 (1974).
 [3] J. P. Pouget, et al. Phys. Rev. Lett. **35**, 873 (1975).
 [4] A. Zylbersztein and N. Mott, Phys. Rev. B **11** (1975).
 [5] C. Sommers and S. Doniach, Solid State Commun. **28**, 133 (1978).
 [6] T. M. Rice, H. Launois, and J. P. Pouget, Phys. Rev. Lett. **73**, 3042 (1994).
 [7] J. Goodenough, J. Solid State Chem. **3** (1971).
 [8] V. Eyert, Ann. Phys. (Leipzig) **11**, 9 (2002).
 [9] R. M. Wentzcovitch, W. Schulz, and P. Allen, Phys. Rev. Lett. **72**, 3389 (1994).
 [10] For recent reviews see G. Biroli, O. Parcollet, and G. Kotliar (2003), cond-mat/0307587 ; T. Maier, M. Jarrell, T. Pruschke, and M. Hettler (2004), cond-mat/0404055 ; A. Lichtenstein, M. Katsnelson, and G. Kotliar (2002), cond-mat/0211076 .
 [11] O. Andersen and T. Saha-Dasgupta, Phys. Rev. B **62**, 16219 (2000).
 [12] M. Laad, L. Craco, and E. Müller-Hartmann, cond-mat/030486 (2003) and 0409027 (2004).
 [13] A. Liebsch and H. Ishida, cond-mat/0310216 (2003).
 [14] E. Pavarini, et al. Phys. Rev. Lett. **92**, 176403 (2004).
 [15] A. Poteryaev, A. Lichtenstein, and G. Kotliar, Phys. Rev. Lett. **93**, 086401 (2004).
 [16] K. Okazaki, et al. Phys. Rev. B **69**, 165104 (2004) ; K. Okazaki, PhD thesis, University of Tokyo (2002).
 [17] T. Koethe, Z. Hu, C. Schüßler-Langeheine, O. Tjernberg, F. Venturini, N. Brookes, W. Reichelt, and L.H. Tjeng (2004), private comm. and to be published.
 [18] S. Shin, et al. Phys. Rev. B **41**, 4993 (1990).